doi:10.1016/j.ymthe.2005.08.008

ARTICLE

Long-Term Restoration of Rod and Cone Vision by Single Dose rAAV-Mediated Gene Transfer to the Retina in a Canine Model of Childhood Blindness

Gregory M. Acland,[1,*] Gustavo D. Aguirre,[2] Jean Bennett,[2] Tomas S. Aleman,[2] Artur V. Cideciyan,[2] Jeannette Bennicelli,[2] Nadine S. Dejneka,[2] Susan E. Pearce-Kelling,[1] Albert M. Maguire,[2] Krzysztof Palczewski,[3] William W. Hauswirth,[4] and Samuel G. Jacobson[2]

[1]*Cornell University, Ithaca, NY 14853, USA*
[2]*University of Pennsylvania, Philadelphia, PA 19104, USA*
[3]*University of Washington, Seattle, WA 98195, USA*
[4]*University of Florida, Gainesville, FL 32611, USA*

**To whom correspondence and reprint requests should be addressed at the Baker Institute, Cornell University, Hungerford Hill Road, Ithaca, NY 14853, USA. Fax: +1 (607) 256 5608. E-mail: gma2@cornell.edu.*

The short- and long-term effects of gene therapy using AAV-mediated RPE65 transfer to canine retinal pigment epithelium were investigated in dogs affected with disease caused by RPE65 deficiency. Results with AAV 2/2, 2/1, and 2/5 vector pseudotypes, human or canine RPE65 cDNA, and constitutive or tissue-specific promoters were similar. Subretinally administered vectors restored retinal function in 23 of 26 eyes, but intravitreal injections consistently did not. Photoreceptoral and postreceptoral function in both rod and cone systems improved with therapy. In dogs followed electroretinographically for 3 years, responses remained stable. Biochemical analysis of retinal retinoids indicates that mutant dogs have no detectable 11-*cis*-retinal, but markedly elevated retinyl esters. Subretinal AAV-RPE65 treatment resulted in detectable 11-*cis*-retinal expression, limited to treated areas. RPE65 protein expression was limited to retinal pigment epithelium of treated areas. Subretinal AAV-RPE65 vector is well tolerated and does not elicit high antibody levels to the vector or the protein in ocular fluids or serum. In long-term studies, wild-type cDNA is expressed only in target cells. Successful, stable restoration of rod and cone photoreceptor function in these dogs has important implications for treatment of human patients affected with Leber congenital amaurosis caused by RPE65 mutations.

Key Words: retinal degeneration, gene therapy, RPE65 protein, dogs, Leber congenital amaurosis, viral vectors

INTRODUCTION

Leber congenital amaurosis (LCA) comprises a group of incurable human early onset genetic retinal degenerative diseases arising from many different molecular defects [1–3]. One form of LCA is caused by mutation of the *RPE65* gene, which encodes a protein of the retinal pigment epithelium (RPE) with a key role in the cycling of retinoids [4–6]. A genetically engineered murine model and naturally occurring canine and murine models with *RPE65* deficiency have been studied and used in different treatment strategies [7–16].

Dramatic restoration of vision with gene therapy was first reported in the canine model of *RPE65*-associated LCA [7]. The initial investigation involved three homozygous $RPE65^{-/-}$ affected dogs that each received a surgically delivered subretinal injection of recombinant adeno-associated virus serotype 2 (AAV2/2) carrying a chicken β-actin-promoter/CMV enhancer-driven wild-type canine *RPE65* cDNA. These results prompted significant questions in anticipation of translating this preclinical work to humans with *RPE65*-associated LCA [17].

The proof-of-principle experiment was confirmed [12,18,19], but questions remain about the magnitude and predictability of a single AAV-RPE65 subretinal treatment, the photoreceptor types treated, the long-term stability of visual improvement after a single treatment, and morphological and biochemical recovery. The

1525-0016/$30.00

doi:10.1016/j.ymthe.2005.08.008

present multidisciplinary study aims to answer such questions in a large group of *RPE65*$^{-/-}$ affected dogs treated with gene replacement therapy.

Results and Discussion

In the majority of cases the vector was well tolerated. In four dogs (seven eyes) intraocular inflammation developed following subretinal (six eyes) or intravitreal (one eye) injection (see Table 1). Protein gel electrophoresis demonstrated that the vector preparation that caused the severe ocular inflammation had not been adequately purified (Supplementary Fig. 1). One of these dogs (BR45) was terminated 7 days postinjection; the intraocular inflammation in the remaining three dogs was controlled with medical treatment (short-term systemic and topical corticosteroids and nonsteroidal anti-inflammatory drugs and topical mydriatics). The eyes of all other dogs in the study, and the eyes of these three dogs after this initial period, have remained asymptomatic for study periods ranging from 6 months to longer than 4 years.

Short-Term Restoration of Rod and Cone Function in a Large Cohort of *RPE65*$^{-/-}$ Affected Dogs

Electroretinogram (ERG) responses, from 26 eyes of 17 *RPE65*$^{-/-}$ affected dogs treated with a single subretinal AAV-RPE65 vector injection, were first evaluated 1–3 months postinjection and compared to ERGs of 45 untreated eyes of 23 *RPE65*$^{-/-}$ affected dogs ages 2–11 months and, in 13 of the dogs, to pretreatment ERGs (Figs. 1A–1C). ERGs evaluated include those reanalyzed from 2 dogs previously published [7] and now followed for 3 years after treatment. In normal dogs ($n = 9$, ages 2–7 months), standard white flashes (0.4 log scot-cd s m^{-2}) evoke ERGs dominated by rod photoreceptor and postreceptoral activity under dark-adapted conditions (Fig. 1A, black traces). A cone system component can be estimated with the use of a rod-desensitizing background light or by presentation of flashes at a flicker rate (29 Hz) that is too fast for the sluggish rod system to follow; both estimates are similar in amplitude and time course (Fig. 1A, red traces). *RPE65*$^{-/-}$ affected dogs without treatment, or with intravitreal AAV-RPE65, show no detectable ERGs for this level of stimulation, whereas subretinal AAV-RPE65 can result in rod and cone ERGs that are normal in waveform but smaller in amplitude (Fig. 1A). We studied function at the level of rod and cone photoreceptors more precisely with higher energy flashes that saturate the leading edge of the ERG [20]. In normal dogs, use of a 2000-fold higher flash energy (3.7 log scot-cd s m^{-2}) evokes leading edges that saturate in amplitude and peak near 4 ms (Fig. 1B). In this early phase of the waveform, dark-adapted responses are dominated by rod photoreceptor activity, which results in amplitudes >10 times larger than the cone photoreceptor component [20]. Light-adapted responses are dominated by the cone system because normal dog rods are severely desensitized in this condition [20]. Amplitudes at these very early times (~4 ms) originate directly from cone photoreceptor activity [21–23].

RPE65$^{-/-}$ affected dogs under dark-adapted conditions showed small but detectable a- and b-wave ERG components (Fig. 1B). Light-adapted waveforms were unchanged from those recorded under dark-adapted conditions and, unexpectedly, they could have *larger* a- and b-waves than normal dogs (Fig. 1B). The a-wave was exceedingly slow, peaking near 10 ms; a response was not detectable at the normal time to peak near 4 ms (Fig. 1B). With intravitreal delivery of AAV-RPE65, ERG shape or amplitude was unchanged. Subretinal delivery of AAV-RPE65, on the other hand, caused major changes; large signal amplitudes could be measured at 4 ms under dark- and light-adapted conditions, consistent with restoration of normal rod and cone photoreceptor sensitivity in a portion of the retina. The b-waves in the subretinally treated eyes appear to be a combination of appropriately scaled normal and *RPE65*$^{-/-}$ affected ERGs. Counterintuitively, ERG photoresponse b-waves in treated eyes could be *smaller* under light-adaptation compared to untreated eyes (Fig. 1B).

The ability to detect significant change in an ERG measure with intervention depends primarily on the expected signal-to-noise ratio (SNR) of that measure. We chose two measures with similar SNRs (~40 dB) to evaluate functional recovery of rod and cone systems: the amplitude of the dark-adapted photoresponse at 4 ms for rod function and the amplitude of light-adapted 29-Hz ERG for cone function (Fig. 1C). None of the 11 intravitreally injected eyes but 23 of 26 subretinally injected eyes showed treatment success for rod or cone function when using a conservative criterion of mean + 3 SD (Fig. 1C). The conclusions were unchanged considering rod postreceptoral responses (which also had a similar SNR) as estimated by the b-wave amplitude of the lower intensity stimulus presented in the dark (data not shown). A cone photoresponse could be demonstrated upon subretinal treatment in 8 of the 23 eyes (data not shown); a result consistent with significantly lower SNR (~20 dB) of this measure compared to the other three measures.

Rod and cone ERGs showed a range of amplitudes in the 23 *RPE65*$^{-/-}$ affected eyes that met criteria for treatment success. Twenty eyes had tapetal (superior) or nontapetal (inferior) locations of the injections; 3 eyes had injections that straddled the two zones. We asked whether ERG amplitude was related to subretinal injection location and area of the visible detachment (bleb) documented at surgery and quantified relative to the area of the tapetum. The bleb areas in the tapetal retina were on average about half as large (mean $\pm$ SD = 0.35 $\pm$ 0.12) as those in the nontapetal zone (0.69 $\pm$ 0.26). ERG

doi:10.1016/j.ymthe.2005.08.008

amplitudes in the 10 eyes with tapetal injections were on average higher (rod 43.8 ± 26.5 μV, cone 8.0 ± 6.2 μV) than those in the 10 eyes with nontapetal injections (rod 28.5 ± 13.3 μV, cone 5.6 ± 2.5 μV). Rod ERG amplitude as a function of the subretinal injection area was much larger in the superior (tapetal) retina compared to the inferior retina (124.7 ± 46.4 versus 44.9 ± 22.8 μV/tapetal area, $P < 0.01$). The two groups of eyes with different injection sites were similar in terms of other parameters (age at injection, vector serotype, promoter, dose, and volume). Taken together, these regional retinal differences between treatment responses suggest a predictable behavior based on different photoreceptor densities in these retinal areas [24].

Long-Term Restoration of Rod and Cone Function

Two dogs from the previous proof-of-principle study [7] had yearly ERG recordings to determine the long-term functional consequences of single subretinal and intravitreal injections. ERGs recorded at 1, 2, and 3 years after the unilateral subretinal injection of AAV-RPE65 in BR33 demonstrate the stability of the functional rescue (Figs. 1D and 1E). Specifically, rod and cone ERG responses to a 0.4 log scot-cd s m^{-2} flash were undetectable before treatment, became sizeable posttreatment, and have remained so for 3 years. Near normal sensitivity was restored to a fraction of rod and cone photoreceptors across the retina, as demonstrated by responses at the 4-ms time point, and these responses were stable through 3 years of follow-up (Fig. 1E). The results were similar in BR47, the second dog with unilateral subretinal treatment (Fig. 1F). Over this period, ERG responses from the intravitreally injected fellow eye of both these dogs were stable and remained within the range expected from untreated *RPE65*$^{-/-}$ affected eyes.

11-*cis*-Retinal is Localized to Treated Retinal Regions

In samples of retina plus RPE/choroid from normal canine eyes, the major retinoid component was 11-*cis*-retinal (2.8 and 2.6 nmol/eye in two dogs). Minor components included retinyl esters (<100 pmol), all-*trans*-retinal (<250 pmol), and all-*trans*-retinol (<250 pmol). In the two normal eyes, there appeared to be no major differences in rhodopsin content (as measured by 11-*cis*-retinal) and no differences in the accumulation of retinyl esters in the different retinal regions sampled, although the superior central sector did have about twice the rhodopsin content of other regions.

Samples of retina plus RPE/choroid from eyes of *RPE65*$^{-/-}$ affected dogs, either untreated or after intravitreal injections of AAV-RPE65, had retinyl ester content that was dramatically (1000- to 10,000-fold) elevated compared to normal controls. This increase appeared age dependent (1.4–2.2 nmol/eye for BR132 (age 3 months) and 35 ± 8 nmol/eye for other dogs (ages 10 to 25 months); Figs. 2A–2C, Supplementary Table 1).

Samples of retina plus RPE/choroid from eyes of *RPE65*$^{-/-}$ affected dogs, either untreated or after intravitreal injections of AAV-RPE65, had no measurable 11-*cis*-retinal. Recovery, assessed by the presence of 11-*cis*-retinal, occurred in eyes that had received subretinal injections of AAV-RPE65 (Supplementary Table 1). The recovery was not diffuse across the retina but restricted to the region of the subretinal injection (Fig. 2D, Supplementary Table 1). There was no significant amount of 9-*cis*-retinal. The small amounts detected are likely the product of isomerization during sample preparation and they are well below recovered 11-*cis*-retinal production. (The small peak marked with the blue arrow could not be positively identified as 9-*cis*-retinal oxime [25].) There were no dramatic differences in retinyl ester levels in the recovered retinal regions compared to surrounding regions within 14 months posttreatment.

In four eyes of two *RPE65*$^{-/-}$ affected dogs (BR74, BR111; Supplementary Table 1), we assessed functional retinal recovery by both retinoid content and ERG function. In one eye of each animal (BR74OD, BR111OS), the subretinal injection was in the superior tapetal retina. Based on rod and cone function, we considered these two eyes treatment successes. Retinoid results were concordant; and the superior retinal location of detectable 11-*cis*-retinal was consistent with the site of subretinal injection (see above and Supplementary Table 1). The right eye of BR111 had an intravitreal injection of AAV-RPE65 and showed no difference in rod and cone function or retinoids compared with untreated *RPE65*$^{-/-}$ affected dogs. The left eye of BR74, however, had an inferior subretinal injection of AAV-RPE65 and rod and cone function did not meet the criteria established for treatment success. Retinoid analyses, however, detected inferior retinal 11-*cis*-retinal, at about 10-fold fewer pmol/area than the highest amounts found in the superior retina of BR74OD or BR111OS. This suggests that at least one of the three eyes not appreciable as a treatment success by full-field rod and cone functional analyses did have measurable although lesser success, as assayed by the retinoid analyses.

Preservation of Photoreceptor Structure and Expression of RPE65 in Treated Eyes

Young, affected untreated dogs showed only two abnormalities: very slight disorganization of the photoreceptor outer segments and the accumulation of lipoidal inclusions in the RPE. Photoreceptor length was normal, and there was no photoreceptor degeneration or cell loss present at this age (Fig. 3, compare 3A and 3B with 3C and 3D). The RPE lipid inclusions were distinct and increased in size and number with age, but their distribution throughout the monolayer was not uniform.

ARTICLE

doi:10.1016/j.ymthe.2005.08.008

TABLE 1: Summary of dogs and studies

Dog ID	Eye	Tx	Age at Tx (weeks)	Vector	Dose	Vol	Subretinal bleb location	Reaction	Follow up period	Studies				
										ERG	Morphology	Immunohisto-chemistry	Retinoids	PCR
BR29	L	1	37	1			T		*		+			
BR29	R	1	19	1	3.9	150	T		***	+				
BR33	L	2	18	1	3.7	150	na		****	+				
BR33	R	1	18	1	4.6	200	Nt		****	+				
BR45	L	1	33	1	4.6	200	T	+	*		+			
BR45	R	0	na	na			na			+				
BR46	L	0	na	na			na			+				+
BR46	R	0	na	na			na			+				+
BR47	L	2	15	1			na		****	+				
BR47	R	1	15	1	4.6	200	Nt		****	+				
BR53	L	1	46	1	4.6	200	T		**	+	+	+		
BR53	R	1	46	1	11.7	100	T/Nt		**	+	+	+		
BR58	L	1	50	1	11.7	100	T/Nt	+	****	+				
BR58	R	1	50	1	8.7	150	Nt	+	****	+				
BR61	L	2	43	1	8.7	150	na		**	+	+	+		
BR61	R	1	43	1	11.7	100	Nt		**	+	+	+		
BR74	L	1	31	1	11.7	100	Nt	+	**	+			+	
BR74	R	1	31	1	3.9	150	T	+	**	+			+	
BR75	L	2	57	2	3.9	150	na		*	+	+			
BR75	R	1	57	2	100	250	Nt	+	*	+	+	+		
BR76	L	2	31	1	100	250	na	+	**	+				+
BR76	R	1	31	1	3.9	150	T		**	+				+
BR81	L	1	29	1	3.9	150	T		**	+	+			+
BR81	R	1	29	1	11.7	150	Nt		**	+	+			
BR85	L	2	56	3	11.7	150	na		*	+	+			
BR85	R	2	56	3	100	250	na		*	+	+	+		
BR111	L	1	47	2	100	250	T		***	+			+	
BR111	R	2	47	3	100	250	na		***	+			+	
BR113	L	0	na	na	100	250	na				+	+		
BR113	R	0	na	na			na				+			
BR114	L	2	45	2			na		*	+	+	+		
BR114	R	2	45	2	100	250	na		*	+	+			
BR117	L	1	45	2	100	250	Nt		***	+	+	+		
BR117	R	1	45	3	100	250	T/Nt		***	+	+	+		
BR119	L	2	16	1	100	250	na		**	+	+			
BR119	R	1	16	1	11.7	150	Nt		**	+	+			
BR122	L	0	na	na	11.7	150	na							+
BR122	R	0	na	na			na						+	
BR158	L	1	26	4			A		***	+	+	+		
BR158	R	1	26	4	200	150	Nt		***	+	+	+		
BR161	L	1	24	4	160	250	Nt		***	+	+	+		
BR161	R	1	24	4	160	250	T		***	+	+	+		
BR164	L	1	24	5	70	110	T		***	+	+	+		
BR164	R	1	24	5	207	250	Nt		***	+	+	+		
BR174	L	1	16	5	207	250	T		***	+	+	+		
BR174	R	1	16	5	100	200	T		***	+	+	+		
BR140	L	0	na	na	100	200	na						+	
BR140	R	0	na	na			na						+	
BR132	L	0	na	na			na						+	
BR132	R	0	na	na			na						+	
BR82	L	1	27	1			T		*		+			+
BR82	R	2	27	1	11.7	200	na		*		+			
BR89	L	0	na	na	11.7	200	na				+	+		
BR89	R	0	na	na			na				+			

doi:10.1016/j.ymthe.2005.08.008

TABLE 1 (*continued*)

Dog ID	Eye	Tx	Age at Tx (weeks)	Vector	Dose	Vol	Subretinal bleb location	Reaction	Follow up period	Studies				
										ERG	Morphology	Immunohisto-chemistry	Retinoids	PCR
BR118	L	0	na	na			na				+	+		
BR118	R	0	na	na			na				+			
BR129	L	0	na	na			na				+	+		
BR129	R	0	na	na			na				+			
Exp1817	L	0	na	na			na				+			
Exp1817	R	0	na	na			na				+			
Exp2818	L	0	na	na			na				+			
Exp2818	R	0	na	na			na				+			

All dogs used in study are listed, except for 9 normal dogs tested as electroretinography (ERG) controls. Dog ID, all dogs except BR140 were affected (RPE65$^{-/-}$); BR140 was an unaffected control. Dogs Exp1817 and Exp2818 were purebred briard dogs; all others were mixed-breed research colony-bred dogs derived from a single affected briard. Total number of dogs in study was 31 (62 eyes). L, left eye; R, right eye. Tx: 1, 29 eyes received subretinal vector; 2, 12 eyes received intravitreal vector; 0, 21 eyes were untreated controls. Vector: 1, AAV2/2-CBA-cRPE65; 2, AAV2/5-CBA-hRPE65; 3, AAV2/2-CBA-hRPE65; 4, AAV2/1-CBA-hRPE65; 5, AAV2/1-RPE08-hRPE65. Dose, total dose of vector administered in units of 10^6 viral genomes. Volume, injection volume in μl. Subretinal bleb location: T, superior; tapetal region, Nt, inferior; nontapetal region, T/Nt, across tapetal–nontapetal boundary. Reaction indicates (+) 7 eyes that developed inflammatory reaction to inadequately purified vector. Follow-up period ranks time from therapy to most recent evaluation: *, >2, <6 months; **, >6months, <1 year; ***, >1, <2 years; ****, >3.5, <5.5 years. Studies identifies eyes studied (+) by ERG;retinal immunohistochemistry, analysis of retinal retinoids, and/or molecular analysis (PCR). na, not applicable.

Older affected dogs showed similar photoreceptor changes in the superior tapetal region. In the nontapetal region, however, the photoreceptor abnormalities were more severe; there was outer segment shortening and disorganization and loss of one or two rows of nuclei from the outer nuclear layer (data not shown). Unlike the normal retina, which showed very intense and uniform labeling limited to the RPE with the anti-RPE65 antibody, the mutant RPE was not labeled (Fig. 3, compare 3G and 3H with 3I and 3J); the opsin antibody and peanut agglutinin (PNA) lectin gave similar labeling results in normal and mutant retinas (Figs. 3G–3J).

Eyes receiving intravitreal vector injections showed no RPE65 immunolabeling in the RPE or retina, and the retinal structure was similar to that of the untreated eyes of similar age or untreated areas of eyes receiving subretinal vector. Inner retinal layers, particularly the ganglion cell layer, showed no RPE65 labeling. In contrast, eyes receiving subretinal vector showed very distinct RPE65 labeling limited to the RPE cells of the treated area (Figs. 3K, 3L, 3P, 3R, 3T, 3V; Supplementary Fig. 2 (movie)). With two exceptions, no other cells showed RPE65 protein expression after treatment. In one dog, there was multifocal labeling of tapetal cells (data not shown); in a second dog, one rod cell showed diffuse RPE65 cytoplasmic labeling (Figs. 3M and 3N). Treated areas showed normal morphology of photoreceptor outer segments in both the tapetal and the nontapetal regions (Figs. 3E and 3F). Because of the variability in size and number of lipid inclusions, and the limitations of analysis using conventional retinal sections, we did not attempt to determine if treatment resulted in changes in the size and number of these inclusions. There were no appreciable differences in the thickness of the nuclear layers for comparable regions of normal, affected, and treated affected retinals (Fig. 3; Supplementary Fig. 2), which reflects both an absence of untoward effect of therapy and the very slow course of the natural disease.

RPE65 immunolabeling following subretinal injections was limited to the treated areas, but the intensity and extent of labeling were not equal in all eyes. In some, the distribution of RPE65 protein was restricted to a small area within the treated regions, while other eyes showed a wider distribution and intensity of RPE65 labeling. In general, eyes that were considered to have a very good bleb following injection had RPE65 labeling that covered a larger area of the treated monolayer and showed more intense labeling. Conversely, eyes with poor postinjection blebs had more restricted and less intense labeling. In one dog (BR53), there were greater amplitudes of rod and cone ERGs in the left eye compared with those of the right eye. In part, this may reflect the larger bleb observed in the left eye (Fig. 3S) compared to the right (Fig. 3O). Correspondingly, RPE65 immunolabeling showed more intense and diffuse RPE labeling in the left eye (Figs. 3S–3V) compared to the right (Figs. 3P–3R). The right eye of BR53 showed some regions with intense immunolabeling (Fig. 3R; Supplementary Fig. 2), which suggests that within such regions functional restoration had been achieved.

Serology

Sera from all dogs studied exhibited increased immunoreactivity with the AAV2/2 antigen compared to serum from the unimmunized pup. Some, but not all, adult dogs had especially high pretreatment immunoreactivity to AAV2/2. For example, BR119 and BR81 had high pretreatment serum antibodies, whereas BR33, BR61, BR122, and BR114 did not. Serum immunoreactivity to AAV2/2 increased in all animals injected intraocularly with AAV2/2-RPE65, but was especially elevated in those animals with high pretherapy serology. Increases were not dependent on site of delivery of AAV-RPE65 (intra-

ARTICLE

doi:10.1016/j.ymthe.2005.08.008

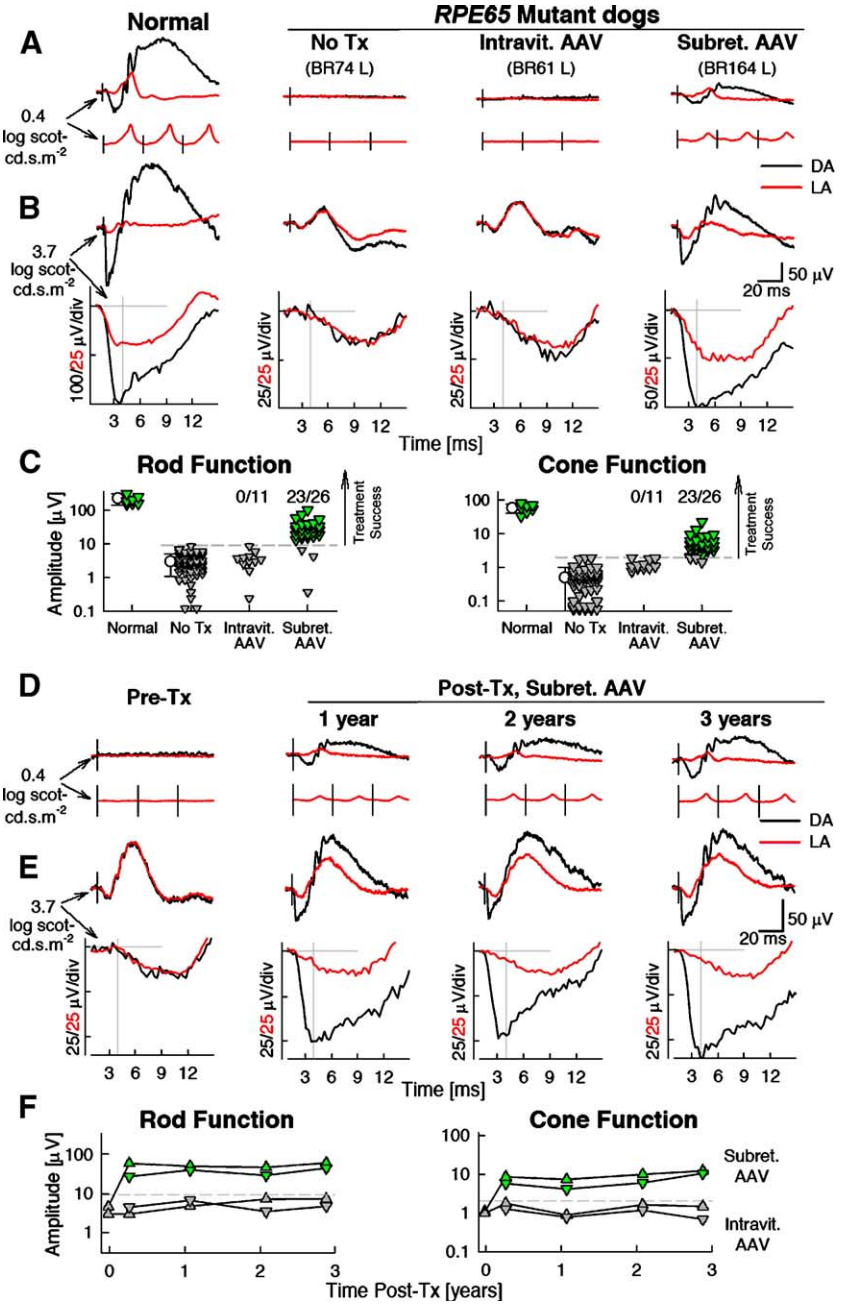

FIG. 1. Short-term (A–C, 1–3 months) and long-term (D–F) restoration of rod and cone retinal function after a single subretinal treatment of AAV-RPE65. (A) Representative ERGs evoked by standard white flashes (0.4 log scot-cd s m^{-2}) presented under dark-adapted (DA) and light-adapted (LA) conditions. DA traces are single flashes, LA traces are averages obtained at repetition frequencies of 1 (top) and 29 Hz (bottom). Black vertical lines show the timing of the flashes. Identities of the dogs (BR74, BR61, BR164) refer to Table 1; R, right eye, L, left eye. ERGs were performed at 3 and 1 months posttreatment in BR61 and BR164, respectively. (B) ERG photoresponses evoked by white flashes of high energy (3.7 log scot-cd s m^{-2}) under DA and LA conditions, same data are shown on slow (top) and fast (bottom) time scales to allow interpretation of late and early components, respectively. Gray lines show the baseline and the 4-ms time point at which rod and cone photoreceptor responses were measured. (C) Comparison of rod and cone function in the control eyes to that of the two treatment groups. Rod function shown refers to the DA ERG photoresponse amplitude at 4 ms and cone function refers to the peak amplitude of the LA 29-Hz waveform. Each triangle represents an eye. Horizontal dashed lines represent the upper limit (mean + 3 SD) of the respective measurement in the group of control *RPE65*$^{-/-}$ affected eyes (n = 47), which had not received treatment (No Tx). Successful recovery of rod and cone function is demonstrable in 23/26 (88%; green triangles) of the eyes receiving subretinal AAV-RPE65 but 0/11 (0%) of the eyes receiving intravitreal AAV-RPE65. Symbols with error bars show the statistics (means ± SD) for the two control groups. (D) ERGs evoked by standard white flashes in the right eye of an RPE65 mutant dog (BR33) before treatment (Pre-Tx) and over a 3-year interval after treatment. Color coding as in B. (E) ERG photoresponses evoked with white flashes of high energy over the same 3-year interval in the same eye as in D. Waveforms displayed as in A and B. (F) Two eyes with subretinal AAV-RPE65 show stable level of partial restoration of retinal rod and cone function, whereas two eyes with intravitreal AAV-RPE65 show amplitudes similar to those of untreated eyes. Horizontal dashed lines represent the upper limit (mean + 3 SD) of the respective measurement in the group of control *RPE65*$^{-/-}$ affected eyes, which had not received treatment.

vitreal versus subretinal). For example, BR85 (which had bilateral intravitreal injections) had (mild) increases similar to those of BR53 (which had bilateral subretinal injections). A comparison of ERG results from two dogs without high pretreatment serum antibodies and the two dogs with high antibodies indicated that there was no major difference in success level.

All intraocular fluid samples lacked immunoreactivity to AAV2/2 prior to treatment. There were only mild increases in immunoreactivity posttreatment in a few of the dogs/eyes (for example, right eye of BR81, both eyes of BR119 and BR53). As expected, there were no significant increases in immunoreactivity of serum or intraocular fluids after intraocular injection of an AAV with a capsid different from that of AAV2/2 (i.e., AAV2/5, AAV2/1).

All sera and intraocular fluid samples tested yielded essentially identical ELISA results for GST versus GST-RPE65 antigen, indicating that there is no specific antibody response to RPE65 antigen. This was true even for samples from animals that had exhibited strong inflam-

doi:10.1016/j.ymthe.2005.08.008

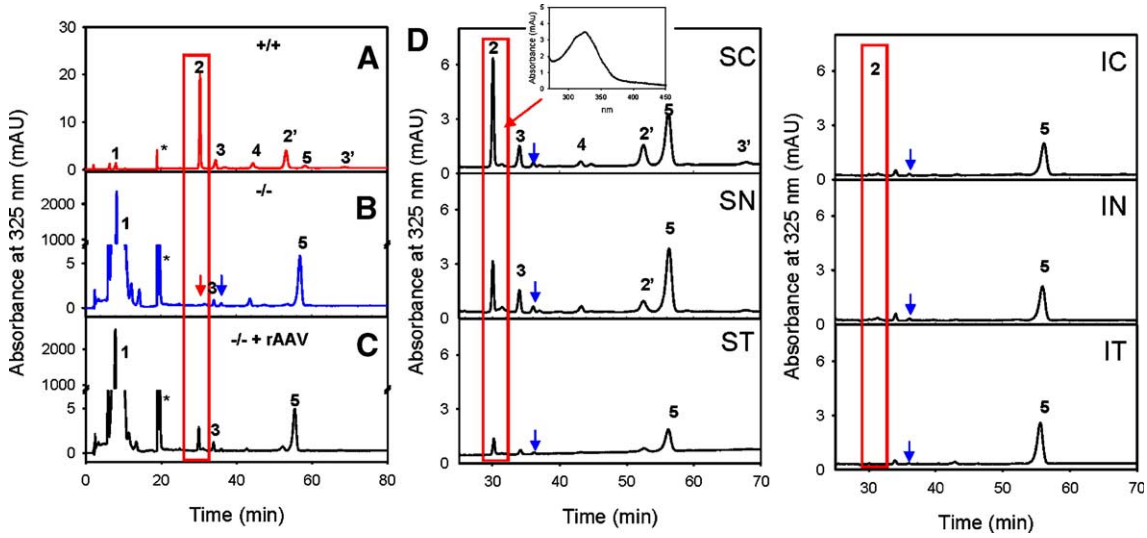

FIG. 2. Chromatographic separation of nonpolar retinoids in retina/RPE–choroid in normal and untreated and treated RPE65$^{-/-}$ dogs. (A) *RPE65*$^{+/+}$ dog (BR140, OS-SC, see Supplementary Table 1). (B) *RPE65*$^{-/-}$ affected dog, untreated (BR122 OD-SC, see Supplementary Table 1). (C) *RPE65*$^{-/-}$ affected dog treated with AAV-RPE65 (BR74 OD; C = SN region). Retinoids were extracted from the indicated regions of the eye and separated on normal-phase HPLC as described under Materials and Methods. The peaks correspond to the following retinoids: 1, all-*trans*-retinyl esters; 2 and 2′, syn- and anti-11-*cis*-retinal oximes; 3 and 3′, syn-all-*trans*-retinal oximes; 4, 11-*cis*-retinol; 5, all-*trans*-retinol. *Artifact related to a change in the solvent composition. The syn isomer of syn-11-*cis*-retinal oxime is shown in the red box; the expected elution time for syn-11-*cis*-retinal oxime is shown by the red arrow; blue arrow indicates expected elution time of syn-9-*cis*-retinal oxime. 11-*cis*-Retinal oximes are present at high level in A, and low level in C, but not in B. There is dramatic accumulation of retinyl esters in the *RPE65*$^{-/-}$affected dog (C) with or (B) without treatment. (D) Regional variation in nonpolar retinoids in six retinal sectors from an eye treated in the superior central retina with rAAV-RPE65. Note the limited diffusion of 11-*cis*-retinal in the treated eye. Its production is restricted to the site of subretinal injection (SC). Inset: The spectrum of peak 2 (syn-11-*cis*-retinal oxime). SC, superior central; SN, superior nasal; ST, superior temporal; I, inferior.

matory responses after ocular gene therapy with AAV-RPE65. Western analysis also yielded no evidence for any specific antibody response to RPE65 in sera or intraocular fluids after subretinal injection of AAV-RPE65 (data not shown), confirming the ELISA results. Continuing studies to examine specifically the results of repeated therapy will address these issues more fully.

Extraocular Transgene Expression

PCR and RT-PCR analyses of frozen tissue from kidney, heart, lung, liver, lymph nodes, bone marrow, ovary/testis, brain (cortex), and extraocular muscle harvested terminally (several months to approximately 1 year posttherapy) revealed no evidence of extraocular presence or expression of the wild-type RPE65 cDNA. Immunocytochemistry revealed no evidence of RPE65 protein in optic nerves of treated dogs (data not shown).

This study confirms and amplifies previous findings that a single dose of subretinally delivered recombinant adeno-associated virus carrying an appropriately promoted wild-type *RPE65* cDNA can restore vision in the canine model of *RPE65*-associated LCA and that intravitreally administered vector does not. The degree of visual restoration as assessed by analysis of electroretinographic responses was not influenced to any obvious extent by either the specific vector used among five different combinations of promoter, vector pseudotype, species (canine, human) of cDNA, or even (over approximately 2 log units) the dose of vector used. It is important to note that 3 of 26 eyes that were considered to have good postinjection blebs did not result in treatment success as assessed by conservative ERG measures of rod and cone function. The reasons for these failures are not clear at this time, but could involve sensitivity of a retina-wide test to detect a focal treatment, leakage of vector out of the bleb, or sub-RPE delivery.

Recovery of retinal function was strictly limited to the treated eye in dogs receiving unilateral subretinal gene therapy. Furthermore, biochemical and immunochemistry data agree that only the area treated directly by subretinal injection regains functional RPE65 expression and 11-*cis*-retinal production. This is also concordant with previous results demonstrating, by genomic PCR, that viral DNA persists only in the neural retina and RPE/choroid of the injected quadrant [7].

Even though we used vector pseudotypes and promoters that potentially target multiple cell types, we observed expression of RPE65 protein, as determined by immunocytochemistry, only in RPE cells, except for one lone rod photoreceptor. Absence of RPE65 protein from canine ganglion cells, in eyes treated subretinally or intravitreally, is concordant with results in mice treated similarly [15], but contrasts with intravitreal injection of

ARTICLE

doi:10.1016/j.ymthe.2005.08.008

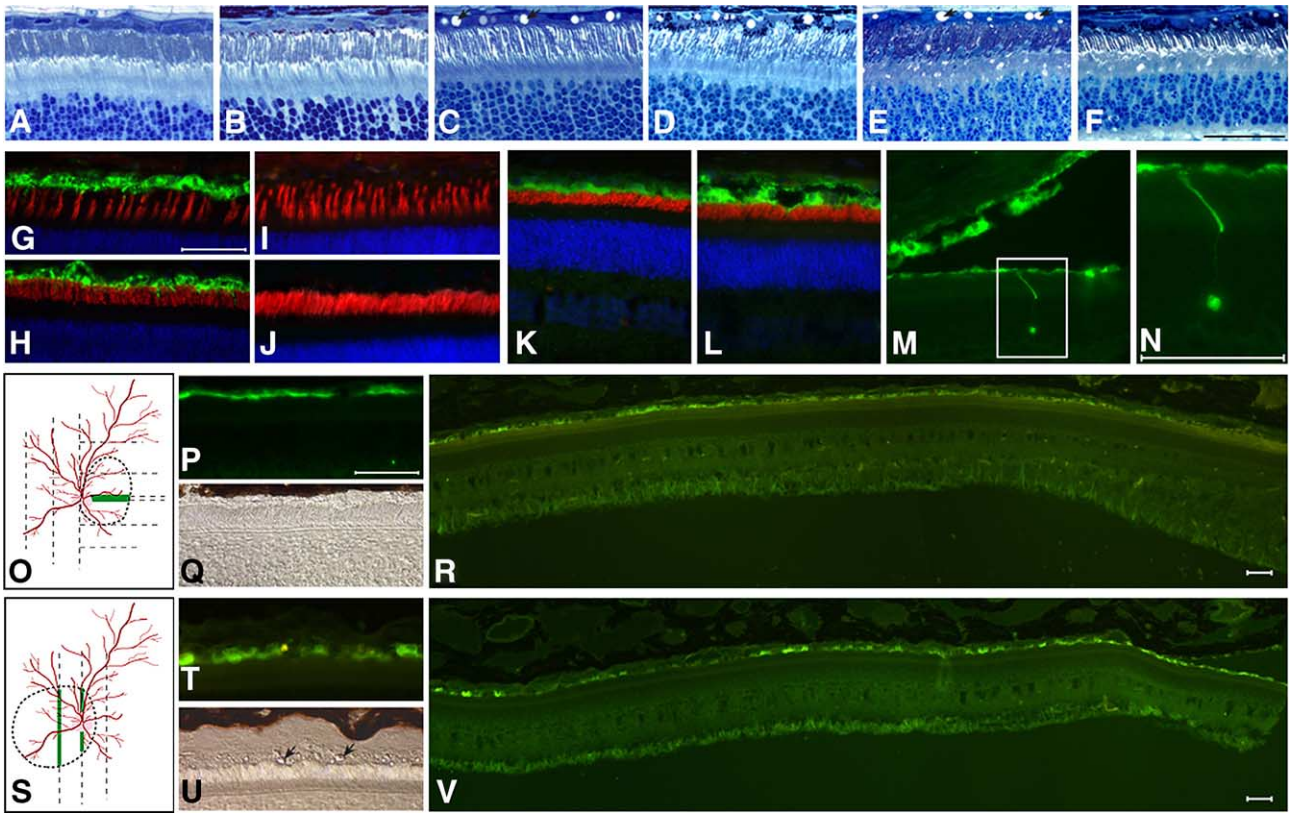

FIG. 3. Retinal photomicrographs of (A, B, G, H) normal, (C, D, I, J) RPE65$^{-/-}$, and (E, F, K–V) vector-treated RPE65$^{-/-}$ dogs. Vector-treated animals were (E, F) BR119, right eye, injected with AAV2/2-CBA-cRPE65 at 3.5 months and sampled at 10.5 months; (K, O–R) BR53, right eye, injected with AAV2/2-CBA-cRPE65 at 10.5 months and sampled at 17.5 months; (L, M, N) BR117, left eye, injected with AAV2/5-CBA-hRPE65 at 10 months and sampled at 2 years; and (S–V) BR53, left eye, injected with AAV2/2-CBA-cRPE65 at 10 months and sampled at 18 months. As in normal (A, B; 5.5 months), the photoreceptor and outer nuclear layers are intact in affected (C, D; 3 months) and in vector-treated animals (E, F). Lipoidal inclusions in the retinal pigment epithelium are prominent in both untreated and treated affected animals (small oblique arrows in C, E). Normal dogs show intense RPE65 immunolabeling (G, H, green), and peanut agglutinin (PNA; G) and opsin (H) label, respectively, the extracellular insoluble cone domains and the rod outer segments. The *RPE65*$^{-/-}$ dog shows the same pattern of labeling with PNA (I) and opsin (J), but RPE65 immunolabeling is absent. In treated animals, opsin immunolabeling (red) remains unchanged, but RPE65 labeling is restored (green) and limited to the RPE layer (K, L). (M) and (N) show low- and high-power views of RPE65 expression in the RPE cell layer and in one rod photoreceptor (green). (O–R) and (S–V) show that, although the distribution of expression is more limited in the right retina (O, R) than in the left (S, V), RPE65 labeling is present in RPE cells but no other cells. Even in areas with intense RPE65 expression, lipoidal inclusions in the RPE are still present (Q, U, small oblique arrows). All calibration markers represent 50 μm, marker in F applies to all except N, R, and V.

AAV.CMV.EGFP, which results in EGFP production in canine and mouse ganglion cells [26]. These results suggest that production of stable RPE65 protein requires a specific cellular environment and that future studies to explore this issue are clearly needed.

Apart from one episode with a batch of vector that was inadvertently incompletely purified (Supplementary Fig. 1), we observed no significant inflammatory or other deleterious effects of the therapy. Moreover, even eyes suffering inflammation from impure vector eventually responded to medication and demonstrated significant restoration of vision. All dogs retained for long-term evaluation have remained healthy, with no medication required after the immediate posttherapy period. Such results are in accord with other safety studies of subretinal rAAV in dogs [27]. At present, one dog is 5 years out from the date of therapy, and six are between 2 and 4 years. These are very significant periods in terms of the canine life span, with no evidence of untoward result of the therapy. The visual recovery assessed by ERG has shown no sign of decrement at the time points measured, indicating that, at the retinal level, the recovery of rod and cone photoreceptor function is stable.

In general, biochemical and immunochemistry results have been congruent with the functional assessment by ERG. Interestingly, in one eye we found biochemical evidence of 11-*cis*-retinal production but no statistically significant difference in ERG parameters in this eye compared with untreated eyes. This observation may have implications for potential therapy monitoring in human patients, if improved visual perception occurs in retinal regions too small to be detected by a full-field

doi:10.1016/j.ymthe.2005.08.008

measurement of retinal function such as the ERG. In anticipation of such treatment effects, strategies have recently been devised to detect small regional changes in visual thresholds in humans with LCA [17,28].

Materials and Methods

Animals. Forty dogs were studied. Twenty-eight dogs homozygous for the canine *RPE65* mutation (Table 1), and 1 unaffected control (Table 1), were part of a research strain of mixed-breed dogs maintained at the Retinal Disease Studies Facility (Kennett Square, PA, USA). The disease in this strain derives from a single affected briard dog and is caused by a 4-bp deletion in the canine *RPE65* gene, as described previously [13]. Molecular diagnostic testing has determined that this strain is homozygous normal for other genes/loci responsible for inherited retinal degeneration in dogs (*prcd, erd, CNGB3, PDE6B, Rho, RPGR*). Two purebred briard dogs (Exp1817, Exp2818; Table 1), affected by the same *RPE65* mutation as the colony dogs, were also studied as affected, untreated controls. In addition, 14 eyes from 9 normal control dogs were used for ERG studies. All procedures involving animals were undertaken in accordance with the guidelines of the U.S. Public Health Service's policy on the humane care and use of laboratory animals. Twenty-nine eyes of 19 affected dogs each received a single subretinal injection containing a therapeutic vector (Table 1); 26 of these eyes (17 dogs) were subsequently tested at least once by ERG. Fourteen eyes of 11 affected dogs (Table 1) received an intravitreal injection of vector, a sham injection, or no injection, and subsequently each of these eyes was also tested at least once by ERG. Eyes were harvested at selected time points posttherapy to evaluate the results of treatment by morphology, immunohistochemistry, retinoid analyses, and molecular studies (Table 1). Thirty-seven eyes from 22 dogs were harvested for morphological evaluation, including 21 for immunohistochemical examination (Table 1). These included 4 eyes from the 2 purebred affected briard dogs and 33 eyes from 20 colony dogs. Eighteen of these eyes had each received a subretinal vector injection, 7 had received an intravitreal injection, and 12 (including the 4 purebred briard eyes) had received no therapy.

Vectors. Five types of therapeutic AAV vectors, identified as AAV2/2-CBA-cRPE65, AAV2/5-CBA-hRPE65, AAV2/2-CBA-hRPE65, AAV2/1-CBA-hRPE65, and AAV2/1-RPE08-hRPE65, were used (Table 1). All vectors are flanked by 143-bp AAV2 inverted terminal repeats and contain a 199-bp SV40 polyadenylation signal sequence. AAV2/2, AAV2/1, and AAV2/5 vectors are packaged into serotype 2, 1, or 5 capsids, respectively. CBA indicates the 1680-bp hybrid chicken β-actin promoter, encompassing a cytomegalovirus immediate early enhancer (381 bp), the proximal chicken β-actin promoter (283 bp), and the chicken β-actin intron 1 flanked by exon 1 and exon 2 sequences [29]. RPE08 is an 823-bp human RPE65-specific promoter (−1 to −822). cRPE65 is a 1656-bp canine RPE65 cDNA, and hRPE65 is a 1602-bp human RPE65 cDNA. AAV2/1-CBA-hRPE65 also contains a 594-bp woodchuck hepatitis virus posttranscriptional element. All AAV vectors were produced and purified identically according to Zolotukhin *et al.* [30,31] but with modifications. HEK 293 cells (ATCC) were cultured in Dulbecco's modified Eagle's medium (DMEM) supplemented with 5% fetal bovine serum and antibiotics. A $CaPO_4$ transfection precipitation was set up by mixing a 1:1 molar ratio of the rAAV vector plasmid and the helper plasmid pDG(4), which contained all the helper functions required for production of the vector, including the desired AAV serotype capsid gene. For serotype 2 vectors the capsid gene was from wild-type serotype 2 AAV; for serotype 1 vector a pseudotyped virus was produced with a helper plasmid containing an AAV serotype 1 capsid gene, and for the serotype 5 vector a pseudotyped virus was produced with helper plasmid containing an AAV serotype 5 capsid gene. For each vector the appropriate two-plasmid DNA precipitate was added to 1100 ml of DMEM and the mixture applied to 293 cell monolayers in a cell factory (Nalge Nunc International, Rochester, NY, USA). The transfection was allowed to incubate at 37°C for 60 h, after which the cells were harvested and lysed by three freeze/thaw cycles. The crude lysate was clarified by centrifugation and the resulting vector-containing supernatant divided between four discontinuous iodixanol step gradients and run at 350,000*g* for 1 h. Five milliliters of each 60–40% step interface was removed, and the combined vector fractions were further purified and concentrated by column chromatography on a 5-ml HiTrap, Q Sepharose column using a Pharmacia ATKA FPLC system. The vector was loaded in 20 mM NaCl, pH 8.0, and eluted from the column using a 500 mM NaCl, pH 8.0, step gradient. The appropriate eluted fractions were then pooled and concentrated and the buffer was exchanged with PBS in a Biomax 100K concentrator (Millipore, Billerica, MA, USA). Vector purity was assessed by silver-stained SDS–polyacrylamide gel electrophoresis [30]. Each vector was titered for physical particles by quantitative competitive PCR [32] and AAV vectors were then stored at −80°C in PBS prior to use.

Surgical procedures and postsurgical treatment and evaluation. Five cubic centimeters of blood for baseline serology studies was collected by venipuncture prior to treatment, and then animals were anesthetized with thiopental/isoflurane. Subretinal injections were performed as described [7,32] after injecting 5–10 cc sterile saline retro-orbitally to prevent rotation of the eye. Briefly, after mydriasis, an anterior chamber paracentesis was performed with a 30-gauge needle to provide space for the vector and to obtain fluid for baseline intraocular antibody measurements. A 30-gauge anterior chamber cannula (Storz) was inserted through a sclerotomy incision and gently pressed against the neural retina at the desired injection site. A dose volume between 100 and 200 μl was delivered subretinally, thereby creating a localized dome-shaped retinal detachment ("bleb"). The vector dose delivered ranged from approximately 10^{10} to 10^{12} particles. The retinal location of the bleb was observed at the time of surgery and documented by indirect ophthalmoscopy, fundus drawings, and photography. Retinal vessels were assessed to ensure that they remained well perfused during and following the procedure. Four milligrams of Kenalog (triamcinolone acetonide; 40 mg/ml; Bristol–Meyers–Squibb, New York, NY, USA) was injected subconjunctivally, and PredG ointment (Allergan Pharmaceuticals, Irvine, CA, USA) was applied to the corneas while the animals recovered from anesthesia. Following surgery, the dogs were monitored by routine clinical ocular examinations using binocular indirect ophthalmoscopy and biomicroscopy after mydriasis (1% tropicamide); flattening of the subretinal bleb or presence of ocular inflammation was recorded. Immediately following surgery, retinal location and extent of the area of subretinal treatment injection, apparent as a bleb at the time of the surgery, was documented with indirect ophthalmoscopy and fundus drawings. The area of the bleb was quantified from the drawings and specified as a (unitless) fraction of the area of a standard tapetal zone. The location of the injection area was specified as superior (tapetal) or inferior (nontapetal) in most cases; in some eyes, however, the injection area was on the boundary between tapetal and nontapetal zones and was specified as such.

Electroretinography. Dogs were dark-adapted overnight and anesthetized as described [7,20]. Pupils were dilated (cyclopentolate, 1%; phenylephrine,10%), and pulse rate, oxygen saturation, and temperature were monitored. Full-field ERGs were recorded with Burian–Allen contact lens electrodes and a computer-based system. Low-energy (10 μs duration; maximum luminance of unattenuated white flash 0.4 log scot-cd s m^{-2}) and high-energy (1 ms duration; maximum luminance of unattenuated white flash 3.7 log scot-cd s m^{-2}) flashes were used under dark-adapted and light-adapted (1.5 log cd m^{-2} at 1-Hz stimulation, 0.8 log cd m^{-2} at 29-Hz stimulation) conditions [7,20].

Retinoid analysis. Dark-adapted dogs were euthanized and enucleated (all procedures performed under dim red light). Retina, separated from RPE, was divided into six sectors, three from the superior tapetal zone and three from the inferior nontapetal zone. Tissue samples were double wrapped in aluminum foil and stored at −80°C until use. All experimental procedures related to the analysis, derivatization, and separation of retinoids were undertaken as described previously for mouse eyes [8,9]

doi:10.1016/j.ymthe.2005.08.008

with minor modifications as described below. Prior to extraction, retinals were derivatized to oximes with hydroxylamine for better separation under our chromatographic conditions. Retinoid analysis was performed on an Agilent 1100 series high-pressure liquid chromatograph (HPLC) equipped with a diode array detector and Agilent Chemstation A.10.01 software. A normal-phase column (Beckman Ultrasphere Si 5μ, 4.6 × 250 mm) and an isocratic solvent system of 0.5% ethyl acetate in hexane (v/v) for 15 min followed by 4% ethyl acetate in hexane for 65 min at a flow rate of 1.4 ml/min at 20°C (total 80 min) with detection at 325 nm were used.

Histopathology and immunocytochemistry. Thirty-seven eyes were studied morphologically from 20 affected dogs, purposely bred for these studies, and 2 affected purebred briard dogs (4 and 10.5 months of age). These included 18 eyes receiving subretinal injections, 7 receiving intravitreal injections, and 12 receiving no therapy (Table 1). Posttreatment intervals ranged from 3.5 months to 2 years. Retinal sections for morphologic studies were prepared using a triple fixation protocol [33] prior to embedding in plastic, a 4% paraformaldehyde fixation for OCT embedding and immunocytochemistry [34], or Bouin's solution followed by processing for standard paraffin embedding and sectioning for histopathological examination and immunochemistry. For treated eyes, plastic- or OCT-embedded tissues were oriented such that the sections extended through the center of the treated area; untreated areas from adjoining and other quadrants were also included for analysis. For immunocytochemical studies, sections from OCT-embedded retinas were labeled with rabbit anti-mouse RPE65 polyclonal antibody (PETLET; gift from Dr. Michael Redmond), monoclonal antibody K16-107C directed at the C-terminal domain of opsin [35], DAPI, and/or PNA to label the insoluble extracellular domain surrounding the cones [36]. Secondary antibodies included goat anti-rabbit IgG conjugated to either Alexa Fluor 488 (green) or Alexa Fluor 568 (red) and goat anti-mouse IgG conjugated to Alexa Fluor 568 (Molecular Probes, Eugene, OR, USA). Sections were examined with a Zeiss Axioplan microscope using epifluorescence and DIC optics. Images were digitally captured (Spot 3.3; Diagnostic Instrument, Inc., Sterling Height, MI, USA) and imported into Adobe PhotoShop (Adobe Systems, San Jose, CA, USA).

Samples for serology, virology, and extraocular transgene expression. Serum samples were obtained from all dogs receiving therapy, immediately prior to surgery, by venipuncture 3 weeks after injection and, again, terminally. Conjunctival swabs for viral isolation were taken at multiple time points following surgery. Following euthanasia with a pentobarbital overdose, eyes that were enucleated for other studies had fluid samples collected from the anterior chamber and vitreous. All samples were stored at −80°C until used for immunology studies.

Immunology: ELISA to determine Anti-RPE65 antibody response after AAV-RPE65 gene therapy. Antigen was prepared from human RPE65 cDNA amplified from plasmid pAAV2.1CMV-hRPE65 [38] using forward primer 5′-AGGAATTCCATGTCTATCCAGGTTGAGCATC-3′ and reverse primer 5′-CAGAATTCTCAAGATTTTTTGAACAGTCCATG-3′. The 1.6-kb product was digested with *Eco*RI and subcloned into pGEX3X (Pfizer, New York, NY, USA), creating an in-frame fusion of hRPE65 with GST. Both GST-hRPE65 and GST (control) proteins were expressed in BL21 Codon-Plus RIL bacteria (Stratagene, La Jolla, CA, USA). Five milliliters of an overnight culture was used to inoculate 200 ml LB broth; bacterial pellets were washed with PBS and resuspended in 20 ml of lysis buffer (5% lithium dodecyl sulfate, 10 mM Tris, pH 8.2) supplemented with protease inhibitors. DNA was removed by passing the lysates over a column of 425–600 μm-sized, acid-washed glass beads (Sigma Chemical Co., St. Louis, MO, USA). Cleared lysates were aliquoted and stored at −80°C. To verify hRPE65 expression, each bacterial lysate was run on a 10% Bis-Tris NuPAGE gel (Invitrogen, Carlsbad, CA, USA) with Mops running buffer and then electroblotted onto Hybond ECL (Amersham, Piscataway, NJ, USA). The blot was probed with 1:1000 diluted rabbit anti-RPE65 antiserum (PETLET), followed by 1:2000 diluted, HRP-conjugated, donkey anti-rabbit immunoglobulin (Amersham) and finally ECL Plus detection reagent (Amersham). A band of approximately 90 kDa was detected in lanes containing GST-RPE65 lysates and was absent in lanes containing only GST lysates. The ELISA validation assay demonstrated that the reaction conditions tested specifically for antibodies to RPE65.

ELISA validation assay. One hundred microliters of antigen (1:100 dilution in 0.1 M sodium bicarbonate, pH 9.6) was aliquoted per well of a 96-well high-binding EIA/RIA plate (Corning, Corning, NY, USA) and incubated overnight at 4°C. After coating with antigen, the wells were blocked with 1% BSA and sequentially incubated with 1:2000 diluted rabbit anti-RPE65 antiserum (PETLET) or control rabbit anti-β-galactosidase antiserum (Chemicon, Temecula, CA, USA), followed by 1:2000 diluted, HRP-conjugated, donkey anti-rabbit immunoglobulin (Amersham) and *p*-phenylenediamine dihydrochloride substrate (Sigma–Aldrich Corp., St. Louis, MO, USA). Between steps, the wells were washed with 0.05% Tween 20 in PBS. The OD_{490} was determined after quenching with H_2SO_4 using a plate reader (Wallac Victor, Perkin–Elmer, Boston, MA, USA).

Analysis of sera, anterior chamber fluid, and vitreous of treated dogs. Samples from all animals were screened for immunoreactivity to RPE65 protein. Serum from an untreated 3-week-old unimmunized puppy was used as a negative control. All samples were stored at −80°C from the time of collection until their use. The GST and GST-RPE65 test antigen preparations as well as LCI-GP parvo/distemper vaccine (positive control; Fort Dodge Animal Health Division of Wyeth) were diluted 1:100 in 0.1 M sodium bicarbonate, pH 9.6, and 100 μl of diluted antigen was aliquoted per well of a 96-well high-binding EIA/RIA plate (Corning) and incubated overnight at 4°C. After being coated with antigen, the wells were blocked with 1% BSA and sequentially incubated with 1:50 diluted specimen and subsequently analyzed as above.

Western blot. To confirm the results obtained by ELISA, sera from positive (AAV-treated; BR29) and negative (untreated and unimmunized puppy) control dogs were used as probes for Western analysis. Results were compared with a blot probed with rabbit anti-RPE65 antiserum. One microliter of each antigen was run in triplicate on a 10% Bis-Tris NuPAGE gel (Invitrogen) with Mops running buffer and then electroblotted onto Hybond ECL (Amersham). The blots were probed with 1:200 diluted dog serum or 1:1000 diluted rabbit anti-RPE65 antiserum; followed by 1:2000 diluted, HRP-conjugated, sheep anti-dog immunoglobulin (Sigma) or donkey anti-rabbit immunoglobulin (Amersham) and ECL Plus detection reagent (Amersham).

Immunology: antibodies to AAV2/2. Samples were analyzed for antibodies to AAV type 2 capsid proteins. Enhanced protein binding ELISA plates (Costar, Corning, NY, USA) were coated for 2 h at room temperature with antigen using 1.8×10^9 particles/well of AAV2/2 in bicarbonate buffer, pH 9.6. Plates were then washed, blocked, and incubated with diluted (1:20, 1:100) serum and intraocular fluid. Saline and serum from an uninjected, unimmunized puppy were used as negative controls. Samples were applied to wells in triplicate and were incubated overnight at 4°C. Human serum containing high levels of anti-AAV2/2 antibodies served as a positive control. Samples were then washed and incubated for 2 h at room temperature with a 1:1000 dilution of alkaline phosphatase-conjugated rabbit anti-dog IgG (Sigma, 100 μl/well). After washing, color was developed using Sigma Fast paranitrophenyl phosphate substrate (Sigma). The plates were read at an optical density at 405 nm.

Molecular analyses of extraocular transgene expression. Sera, samples from conjunctival swabs, and other frozen organ tissues were analyzed for the presence of RPE65 transcript, by RT-PCR, or transgene, by PCR. For RT-PCR studies of frozen extraocular tissues, RNA was extracted from 5–10 mg of tissue using the RNeasy Mini Kit (Qiagen, Inc., Valencia, CA, USA), and RNA (10 ng) was subsequently reverse transcribed and PCR was performed to amplify a segment of the canine RPE65 cDNA. Two sets of primers were used in two different reactions, using the GeneAmp RNA PCR Kit (Applied Biosystems, Foster City, CA, USA). An RT-PCR assay was designed to discriminate wild-type RPE65 transcript from that containing the briard mutation. Forward primer 5′-CATAACGGAATTTGGCACCT-3′ (JB7) and reverse primer 5′-CAGGGGAATTGTACGACGAC-3′ (JB8) amplify a 219-bp

doi:10.1016/j.ymthe.2005.08.008

product from canine cDNA. The forward primer overlaps the briard deletion and amplifies only wild-type RPE65 when the primer is annealed at 10–12°C above its T_m. A second set of primers (5′-CATAACGGAATTTGG-CACCT-3′ (JB5) and 5′-CAGGGGAATTGTACGACGAC-3′ (JB6)) flanks the region containing the briard deletion and amplifies a 396-bp product from both wild-type and mutant RPE65 under the same PCR conditions. PCR was carried out for 40 cycles with annealing at 51°C for 30 s and extension at 72°C for 1 min per cycle with a final extension of 10 min at 72°C. The PCR products were resolved on a 2% agarose gel. Additional PCRs designed to amplify the wild-type AAV REP DNA sequence were performed using primers forward 5′-TCCTTCAATGCGGCCTC-3′ and reverse 5′-TCATCTTCCCCTCCTCC-3′. PCR was carried out for 36 cycles with annealing at 57°C for 1 min and extension at 72°C for 1 min per cycle with a final extension of 10 min at 72°C.

ACKNOWLEDGMENTS

This work was supported by the NIH (U10EY13729, EY06855, EY11123, EY13385, EY13132, EY08061), The Foundation Fighting Blindness, The ONCE International Prize for R&D in Biomedicine and New Technologies for the Blind, Research to Prevent Blindness, Inc., and the Macula Vision Research Foundation. Technical assistance from Amanda Nickle, Gerri Antonini, and the staff at the RDSF and from Pam Hammond and Julie Jordan at Cornell is gratefully acknowledged. We thank Keith Watamura for invaluable graphics support. We are grateful for the critical help of V. Bhuva, A. Cheung, J. P. Van Hooser, M. Batten, and O. Bond. T. M. Redmond generously provided the RPE65 antibody.

RECEIVED FOR PUBLICATION APRIL 27, 2005; REVISED AUGUST 1, 2005; ACCEPTED AUGUST 19, 2005.

APPENDIX A. SUPPLEMENTARY DATA

Supplementary data associated with this article can be found in the online version at doi:10.1016/j.ymthe.2005.08.008.

REFERENCES

1. Hanein, S., *et al.* (2004). Leber congenital amaurosis: comprehensive survey of the genetic heterogeneity, refinement of the clinical definition, and genotype–phenotype correlations as a strategy for molecular diagnosis. *Hum. Mutat.* **23:** 306–317.
2. Preising, M. N., and Heegard, S. (2004). Recent advances in early-onset severe retinal degeneration: more than just basic research. *Trends Mol. Med.* **10:** 51–54.
3. Cremers, F. P., van den Hurk, J. A., and den Hollander, A. I. (2002). Molecular genetics of Leber congenital amaurosis. *Hum. Mol. Genet.* **11:** 1169–1176.
4. Thompson, D. A., and Gal, A. (2003). Vitamin A metabolism in the retinal pigment epithelium: genes, mutations, and diseases. *Prog. Retinal Eye Res.* **22:** 683–703.
5. Baehr, W., *et al.* (2003). The retinoid cycle and retinal disease. *Vision Res.* **43:** 2957–2958.
6. McBee, J. K., *et al.* (2001). Confronting complexity: the interlink of phototransduction and retinoid metabolism in the vertebrate retina. *Prog. Retinal Eye Res.* **20:** 469–529.
7. Acland, G. M., *et al.* (2001). Gene therapy restores vision in a canine model of childhood blindness. *Nat. Genet.* **28:** 92–95.
8. Van Hooser, J. P., *et al.* (2000). Rapid restoration of visual pigment and function with oral retinoid in a mouse model of childhood blindness. *Proc. Natl. Acad. Sci. USA* **97:** 8623–8628.
9. Van Hooser, J. P., *et al.* (2002). Recovery of visual functions in a mouse model of Leber congenital amaurosis. *J. Biol. Chem.* **277:** 19173–19182.
10. Veske, A., *et al.* (1999). Retinal dystrophy of Swedish briard/briard-beagle dogs is due to a 4-bp deletion in RPE65. *Genomics* **57:** 57–61.
11. Redmond, T. M., *et al.* (1998). RPE65 is necessary for production of 11-cis-vitamin A in the retinal visual cycle. *Nat. Genet.* **20:** 344–351.
12. Narfstrom, K., *et al.* (2003). Functional and structural recovery of the retina after gene therapy in the RPE65 null mutation dog. *Invest. Ophthalmol. Visual Sci.* **44:** 1663–1672.
13. Aguirre, G. D., *et al.* (1998). Congenital stationary night blindness in the dog: common mutation in the RPE65 gene indicates founder effect. *Mol. Vision* **4:** 23.
14. Gouras, P., Kong, J., and Tsang, S. H. (2002). Retinal degeneration and RPE transplantation in Rpe65$^{-/-}$ mice. *Invest. Ophthalmol. Visual Sci.* **43:** 3307–3311.
15. Dejneka, N. S., *et al.* (2004). *In utero* gene therapy rescues vision in a murine model of congenital blindness. *Mol. Ther.* **9:** 182–188.
16. Pang, J., *et al.* (2005). Retinal degeneration 12 (rd12): a new, spontaneously arising mouse model for human Leber congenital amaurosis (LCA). *Mol. Vision* **11:** 152–162.
17. Jacobson, S. G., *et al.* (2005). Identifying photoreceptors in blind eyes due to RPE65 mutations: prerequisite for human gene therapy success. *Proc. Natl. Acad. Sci. USA* (online publication ahead of print).
18. Narfstrom, K., *et al.* (2003). In vivo gene therapy in young and adult RPE65$^{-/-}$ dogs produces long-term visual improvement. *J. Hered.* **94:** 31–37.
19. Ford, M., *et al.* (2003). Gene transfer in the RPE65 null mutation dog: relationship between construct volume, visual behavior and electroretinographic (ERG) results. *Doc. Ophthalmol.* **107:** 79–86.
20. Kijas, J. W., *et al.* (2002). Naturally occurring rhodopsin mutation in the dog causes retinal dysfunction and degeneration mimicking human dominant retinitis pigmentosa. *Proc. Natl. Acad. Sci. USA* **99:** 6328–6333.
21. Cideciyan, A. V., and Jacobson, S. G. (1996). An alternative phototransduction model for human rod and cone ERG a-waves: normal parameters and variation with age. *Vision Res.* **36:** 2609–2621.
22. Robson, J. G., Saszik, S. M., Ahmed, J., and Frishman, L. J. (2003). Rod and cone contributions to the a-wave of the electroretinogram of the macaque. *J. Physiol.* **547:** 509–530.
23. Mahroo, O. A., and Lamb, T. D. (2004). Recovery of the human photopic electroretinogram after bleaching exposures: estimation of pigment regeneration kinetics. *J. Physiol.* **554:** 417–437.
24. Kemp, C. M., and Jacobson, S. G. (1992). Rhodopsin levels in the central retinas of normal miniature poodles and those with progressive rod–cone degeneration. *Exp. Eye Res.* **54:** 947–956.
25. Fan, J., Rohrer, B., Moiseyev, G., Ma, J. X., and Crouch, R. K. (2003). Isorhodopsin rather than rhodopsin mediates rod function in RPE65 knock-out mice. *Proc. Natl. Acad. Sci. USA* **100:** 13662–13667.
26. Dudus, L., *et al.* (1999). Persistent transgene product in retina, optic nerve and brain after intraocular injection of rAAV. *Vision Res.* **39:** 2545–2553.
27. LeMeur, G., *et al.* (2005). Postsurgical assessment and long-term safety of recombinant adeno-associated virus-mediated gene transfer into the retinas of dogs and primates. *Arch. Ophthalmol.* **123:** 500–506.
28. Roman, A. J., *et al.* (2005). Quantifying rod photoreceptor-mediated vision in retinal degenerations: dark-adapted thresholds as outcome measures. *Exp. Eye Res.* **80:** 259–272.
29. Daly, T. M., Vogler, C., Levy, B., Haskins, M. E., and Sands, M. S. (1999). Neonatal gene transfer leads to widespread correction of pathology in a murine model of lysosomal storage disease. *Proc. Natl. Acad. Sci. USA* **96:** 2296–2300.
30. Zolotukhin, S., *et al.* (2000). Production and purification of serotype 1, 2 and 5 recombinant adeno-associated viral vectors. *Methods* **28:** 158–167.
31. Zolotukhin, S., *et al.* (1999). Recombinant adeno-associated virus purification using novel methods improves infectious titer and yield. *Gene Ther.* **6:** 973–985.
32. Bennett, J., *et al.* (1999). Stable transgene expression in rod photoreceptors after recombinant adeno-associated virus-mediated gene transfer to monkey retina. *Proc. Natl. Acad. Sci. USA* **96:** 9920–9925.
33. Acland, G. M., and Aguirre, G. D. (1987). Retinal degenerations in the dog: IV. Early retinal degeneration (erd) in Norwegian elkhounds. *Exp. Eye Res.* **44:** 491.
34. Zhang, Q., *et al.* (2002). Different RPGR exon ORF15 mutations in canids provide insights into photoreceptor cell degeneration. *Hum. Mol. Genet.* **11:** 993–1003.
35. Adamus, G., Zam, Z., Arendt, A., Palczewski, K., McDowell, J., and Hargrave, P. (1991). Anti-rhodopsin monoclonal antibodies of defined specificity: characterization and application. *Vision Res.* **31:** 17–31.
36. Mieziewska, K., vanVeen, T., Murray, J., and Aguirre, G. (1991). Rod and cone specific domains in the interphotoreceptor matrix. *J. Comp. Neurol.* **308:** 371.